Advances in Science and Technology Research Journal

Advances in Science and Technology Research Journal, 2026, 20(2), 114–124
https://doi.org/10.12913/22998624/211125
ISSN 2299-8624, License CC-BY 4.0

Received: 2025.08.26
Accepted: 2025.11.15
Published: 2025.12.23

Experimental and analytical approaches for evaluating adhesive overlay joints

Dariusz Kurpisz[1], Maciej Obst[1*], Sebastian Głowiński[2], Tadeusz Szymczak[3]

[1] Poznan University of Technology, ul. Jana Pawła II 24, 60-965 Poznan, Poland
[2] Pomeranian University of Slupsk, ul. Bohaterow Westerplatte 64, 76-200 Slupsk, Poland
[3] Motor Transport Institute, ul. Jagiellonska 80, 03-301 Warsaw, Poland
* Corresponding author's e-maul: maciej.obst@put.poznan.pl

ABSTRACT

The use of bonded joints, which is common across many industrial sectors, is closely tied to rapid advances in design and manufacturing technologies. Modern adhesives enable their application under a wide range of operating conditions and allow high precision due to advanced production processes. Different types of bonded joints can exhibit distinct mechanical properties. The behaviour of such joints highlights the critical role of shear stress in fracture. Traditionally, the mechanical performance of bonded joints is analysed through static testing, which provides fundamental mechanical parameters. However, to obtain a more comprehensive understanding, experimental studies should also include other loading conditions, such as dynamic testing. This paper presents the results of both static and dynamic tests on adhesive overlay joints. The original methodology is proposed for testing adhesive joints under impulse tensile force, resulting in an impact shear stress of the joint, which is the dominant regime. The specimens were manufactured from 1 mm galvanised steel strips and bonded with two types of adhesives: DP490 and Hybrid CX80. They were subjected to static tensile tests and dynamic tensile tests using force impulses with varying energies and strain rates. The study provides detailed static and dynamic characteristics of the tested adhesive joints, offering a practical perspective for engineering applications. The proposed testing method can serve as a diagnostic tool for adhesive joints and other types, such as form-fit joints. This can be used as support for the adhesive joint behaviour and data for modelling, manufacturing, and the trade market.

Keywords: adhesive joint properties, dynamic testing, static and dynamic characteristics.

INTRODUCTION

The experimental and analytical approaches to bonded joints have been the subject of numerous studies. Yang et al. [1] studied two types of adhesive connections – bonded pipe joints under static and dynamic bending – validated using a numerical approach (LS–Dyna). A similar methodology was employed by Gollins et al. [2], who tested two types of bonded connections (methacrylate and epoxy) to assess their static and dynamic behaviour under ballistic loading.

Komorek et al. [3] proposed a modification of a pendulum hammer for impact testing of overlapped bonded joints, obtaining more reproducible results than those from the Block Impact Test.

The influence of external environmental factors, such as humidity and temperature, on the mechanical properties of bonded joints has also been investigated. Balková et al. [4] studied the effects of temperature and cyclic loading on the adhesion and transparency of soda-lime-silica glass and polycarbonate (PC) bonded with a self-adhesive polyurethane (PU) film. They aimed to identify operational conditions in vehicles that could lead to adhesive delamination and glass opacity. Kolář et al. [5] studied cotton-reinforced adhesive lap joints of sheet metal under cyclic loading, using epoxy resin as the binder. The specimens were tested with an overlay near the measurement gauge, and the viscoelastic properties of the joint were observed. The reinforcing fabric was shown

to improve the mechanical performance of adhesive joints under cyclic loading.

Sahin et al. [6] carried out static and fatigue tensile tests on bonded lap joints with varying specimen thicknesses, depending on the adhesive layer thickness. Using DP460 structural adhesive, they produced joints with the AA2024-T3 aluminium alloy, and reported that the ultimate tensile strength increased with greater bond thickness.

Kałuża et al. [7] reported results from an experimental study of the static and fatigue behaviour of bonded joints between CFRP laminate and high-strength steel. Seven methacrylate adhesives were tested, with specimens prepared to create two shear zones. Tichý et al. [8] investigated the influence of cotton fabrics on the mechanical properties of hybrid adhesive joints under static, quasi-static, and fatigue loading. Their results confirmed the positive effect of cotton fibres on ultimate shear strength. Lap joint specimens were subjected to tensile loading, with a hybrid adhesive composed of cotton fibres and epoxy resin. The bond kind for S235J0 structural steel, as an application of the joint for this kind of conventional material, is represented by values of its strength and elongation as a result of the concentration of microparticle filler. For this case, the region was inspected using the SEM technique to detect damage occurrence [5]. Quasi-static experimental studies on the shape of the ends of bonded joints on the load-bearing capacity of the joints made of carbon fiber reinforced plastics (CFRP) and steel [9].

In addition to these studies, other work has focused on hybrid adhesive bonds under cyclic stress (Kolář et al. [5]), stress concentrations at joint edges (Bula et al. [10]), fracture mechanisms of adhesive joints (Xu et al. [11]), and the strength of bonded joints under dynamic loading regimes (Volkov et al. [12]). Maurel-Pantel et al. [13] compared the static and dynamic behaviour of three structural adhesives for space optical applications. They proposed a methodology for assessing adhesive performance under dynamic conditions and found that static and dynamic responses often differ, making correlation challenging. Rahman et al. [14] highlighted that the mechanical parameters of adhesive materials evolve over time. Prolonged loading, particularly in long-term creep tests of thixotropic, room-temperature-cured epoxy adhesives reinforced with nanoparticles, can reduce load-bearing capacity. Wooden bonded specimens were tested under three-point bending.

The results of tests on adhesive joints used to join plastics are presented in [15], where 3D printing was used to produce the joined elements. The experimental tests consisted of static experiments on adhesively bonded overlay specimens.

A methodology for testing bonded lap joints under impact loading was developed using a modified pendulum hammer [16]. In this case, this kind of device was successfully used for riveted and hybrid riveted-bonded joints and the significant effect of adhesive forces on the impact strength of bonded joints was illustrated. This loading case was also used in [17] for attention to wooden building structures made of glued laminated timber. Acceleration values were applied to assess the tested object through root-mean-square analysis and high-speed impact camera photos. At the same time, energy criteria were addressed to estimate peak impact force values and the dynamic surplus coefficient.

Besides, the joint type can be classified as very easy for production; nevertheless, some papers have indicated that this is not trivial when applications are taken into account with respect to safety operations, i.e., the building [18] and automotive branches of industry [19, 20].

For the building sector, the joint problem is strongly related to the size of the building structure [18]. Therefore, for those cases, real-scale studies of adhesive joints and numerical simulations were used. The mechanical tests' results, such as tensile and shear ones, and the double-lap joint experiment, were employed for the modelling. This enabled the determination of the stress distribution in the joint and the identification of plastic zones and areas of decohesion.

In automotive practice, bonded joints are typically located in a few sections of the vehicle, which are then combined with other components to form the final product [20]. For example, in the case of the XJ sedan (X350) and XK coupe Jaguar models, this type of connection is represented by the following values in metres: 116 and 99, respectively [19]. Furthermore, the diagnostic process for identifying defects in the joint type considered is not straightforward, as it cannot be easily captured by inspection using measurement devices that measure physical quantities. Therefore, the X-ray method is employed as an effective technique in such cases. This can be used for vehicle inspection after manufacturing as well as

following a crash test to thoroughly examine the entire body for any damage regions that may appear [20]. Overall, the existing literature emphasises a strong focus on static and fatigue testing of bonded joints, while their dynamic performance has received comparatively less attention. This study addresses this gap by providing new experimental data on the dynamic behaviour of adhesive overlay joints, supported by results from static tests and proposing a few-stage methodology for adhesive testing. For this purpose, two adhesive types were selected: a very special type (DP490) and a typical type (CX80). Concerning the application of adhesive types in general engineering, this paper aims to contribute to and support this field. The scientific contribution is demonstrated through variations in static and dynamic stiffness up to the point of joint decohesion.

DETAILS OF THE EXPERIMENT AND RESULTS

The joint and experimental procedure

The specimens were prepared from two rectangular steel sheet pieces joined with two types of adhesive (Table 1). An overlapping bonded section was created using galvanised steel sheet strips with a thickness of 1.3 mm and a width of 20 mm (Figures 1, 2).

The applied overlap joint, although not ideal and not comprehensive of all issues related to adhesive bonding, has the advantage of being relatively easy to construct. The research methodology proposed in this approach, expanded to include other types of adhesive bonding, will enable a more accurate evaluation of both the method itself and the comparison of different types of adhesive bonding. The specimens with the specified geometry were slightly deviated from the requirements outlined in ASTM D1002 [21] and ISO 4587 [22], was mainly based on the capabilities available to the researchers. Additionally, the analytical tools employed enable measurements of the shape of the adhesive-bonded joint specimen to be obtained independently of the geometry used.

Table 1. Fundamental properties of the adhesives

Name	Symbol	Colour	Density [g/cm^3]
3M DP490	A	Black	1.14
Hybrid CX80	H	Grey	1.59

The joints were made with two adhesives: 3M Epoxy Structural Adhesive DP490 and Hybricx Black CX80. The first type is a high-strength adhesive designed for use in heavy-duty conditions, such as temperatures up to 120 °C, under both static and dynamic loads, and in challenging environmental conditions, particularly in automotive applications. Its shear strength ranges from 23.7 MPa at -55 °C to 1.9 MPa at 150 °C, [23, 24]. The application is suitable for the following material types: aluminium alloy, cold-rolled steel, and galvanised steel grades [25].

The second adhesive is more versatile than the first, as it can be used in both the building and automotive sectors, and is very common in the trade market. It is recommended for creating a strong bond between ceramics, wood, plastics, and concrete, as well as other materials. Its main mechanical properties are: an ultimate tensile strength of 45 MPa and a temperature range from -40 °C to +100 °C [18]. Since the cohesive zones, including the joints, exhibited significant variation in mechanical properties, careful control of the adhesive amount applied to each specimen was essential. Static tensile tests were performed on a Zwick electro-mechanical testing machine at room temperature, with a crosshead displacement rate of 100 mm/min, using a 50 mm gauge length extensometer (Figure 3). Three specimens of each adhesive type were tested

Dynamic tests were performed using a drop tower (Figures 8 and 10). The specimens were subjected to impact loading by a striker weighing 3.78 kg, which struck the reverser bumper and thereby indirectly loaded the joint (Figures 8, 9). Tests were carried out at various impact energy levels, as shown in Figure 10. The striker was released from different heights to generate the necessary kinetic energy at the point of contact with the reverser bumper. The striker-reverser plate collision was quasi-elastic. This assumption stemmed from observing the interaction between the steel striker and the steel reverser (reverser bumper plate) during the contact, and in particular, the rapid loss of contact between the colliding elements. Specimen deformation was recorded with a Chronos high-speed camera. 20 specimens of every kind of adhesive were tested, but not all of the collected data were acceptable for further analysis, and they were selected for the experiment quality.

Galvanised steel sheet flat strips were used as the joined elements, in the as-received state, i.e.

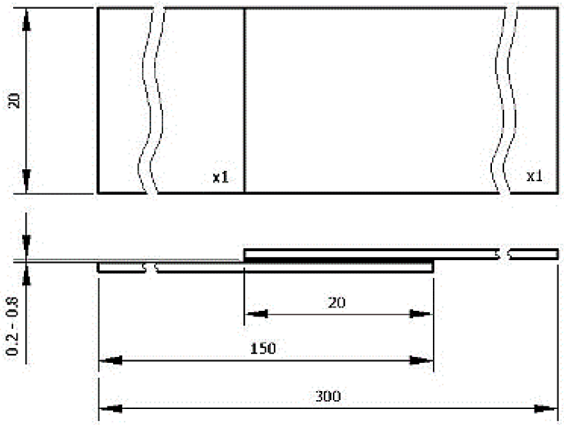

Figure 1. Specimen geometry and dimensions

without surface roughness measurements. The sheet metal where the adhesive was applied was degreased with white spirit. The sheet metal surface was raw and scratched. Specimen strips were cut with sheet metal snips. Care was taken to maintain the same pressure for all specimens during the joining stage (loaded with a wooden beam).

A simple wooden jig was prepared so that one sheet metal strip to be joined was lower than the applied strip by a specified distance. The adhesive was applied manually, ensuring that the wetted surface was contained between the applied sections on the sheet metal.

Static test results

The results are presented as changes in force and displacement (Figures 4 and 5). Applying the approximation using functions family:

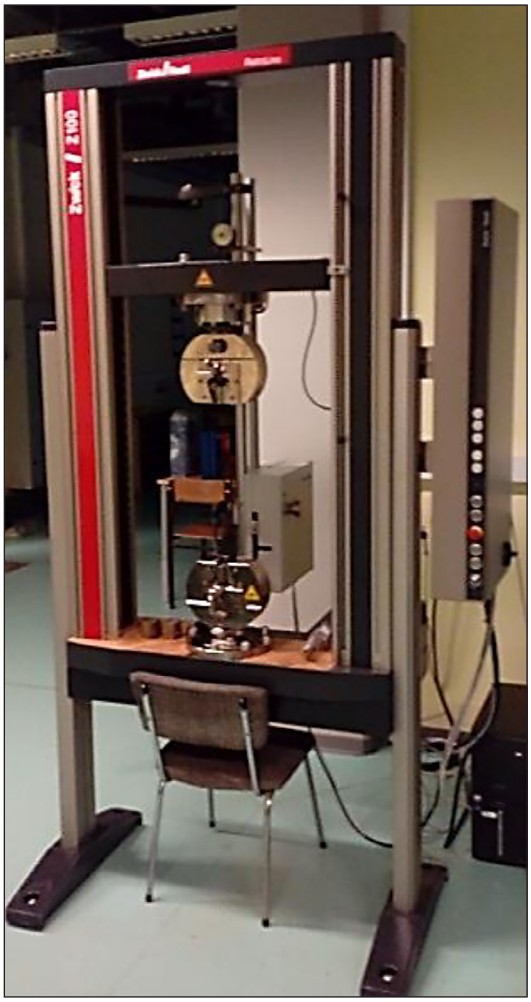

Figure 3. Z100 Zwick electro-mechanical testing machine. Technical features – load capacity: 100 kN; maximum test area: 1070×610 mm^2; crosshead speed range: 0.00005–1000 mm/min; accuracy of the set speed: 0.05; approximate dimensions: 2.0×1.0 m; weight: 450 kg

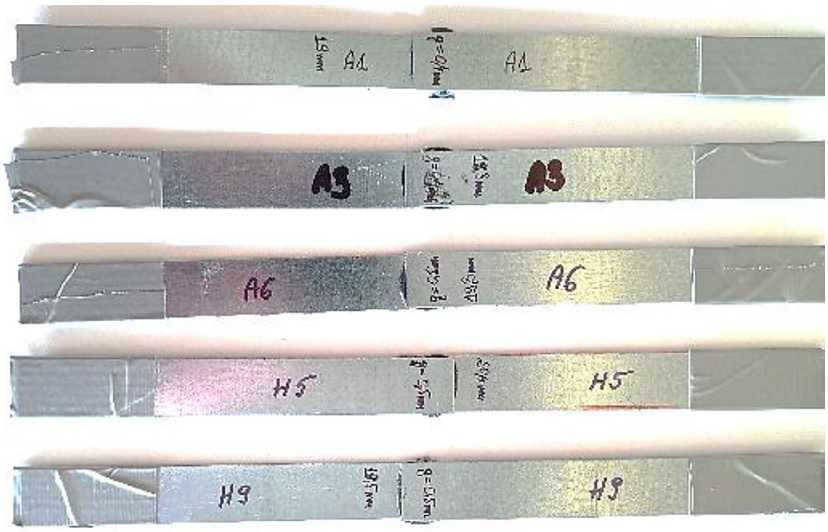

Figure 2. Bonded joint specimens prepared for static and dynamic tests

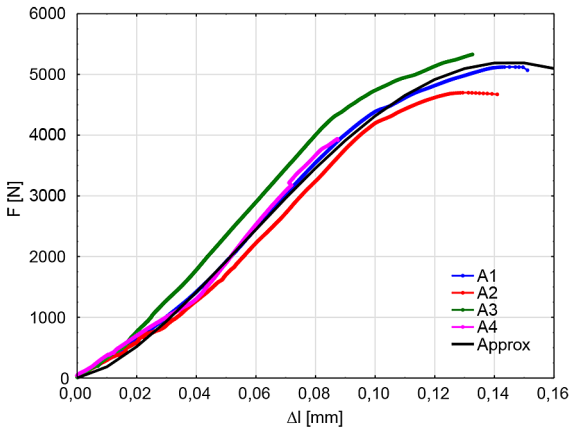

Figure 4. Force versus elongation for the A-bonded specimen joint

$$F(\Delta l) = a \cdot sin^{n}(b\Delta l)\ [N] \quad (1)$$

about coefficients noted in Table 2, the static stiffness changes is proposed in the following form.

$$C(\Delta l) = \frac{anb \cdot sin^{n-1}(b\Delta l) \cdot cos(b\Delta l)}{A} \left[{}^{N}/_{mm} / mm^2 \right] \quad (2)$$

and its mean value can be presented as follows:

$$C_M = \frac{1}{\Delta l_{max}} \cdot \int_0^{\Delta l_{max}} C(\Delta l) d(\Delta l) \quad (3)$$

where: A and Δl_{max} reflect the bonded area and the elongation measure range, respectively.

The obtained graphs and values are presented in Figures 6 and 7 and Table 3. The variations in values of the static stiffness, shown in Figures 6 and 7, reveal two distinct regions determined by the elongation levels. For the A-type joint, this transition occurs at 0.06 mm, while for the H-type joint, it is observed at 0.05 mm. Significant differences were found between the static stiffness maximum values of the joints, indicating that the A-type bonded region exhibits higher mechanical resistance than the H-type. In practice, the static and dynamic stiffness reflect the operation regimes with respect to the elongation values, i.e. in the case of the A-specimen type, this is limited by 0.06 mm, while for the H-type, 0.05 mm holds. It means the component loading for elongation levels higher than the levels can lead to a dramatic lowering of the parameter considered.

Dynamic test results

The influence of tensile energy on the mechanical parameters was evaluated based on

Table 2. Glue types' basic properties

Approximation coefficient	A type glue	H type glue
a [mm]	5200	380
Δl_o [mm]	0.145	0.45
n [mm^{-1}]	10.83	3.49
n	1.50	1.05

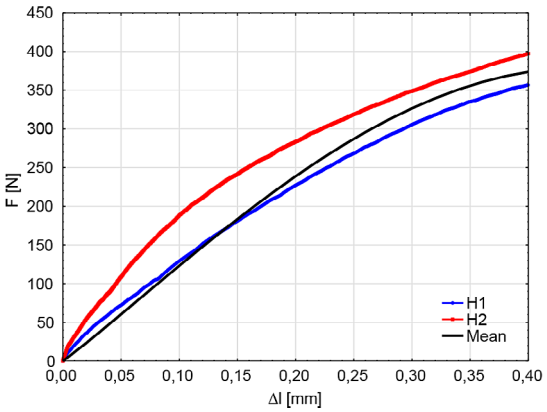

Figure 5. Force versus elongation for the H-bonded specimen joint

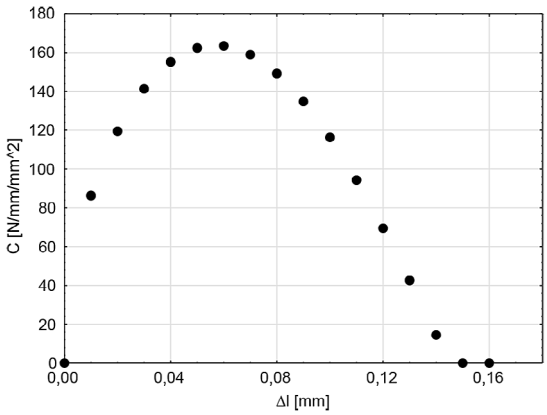

Figure 6. Change in the static stiffness values for the A-specimen type under tensile force

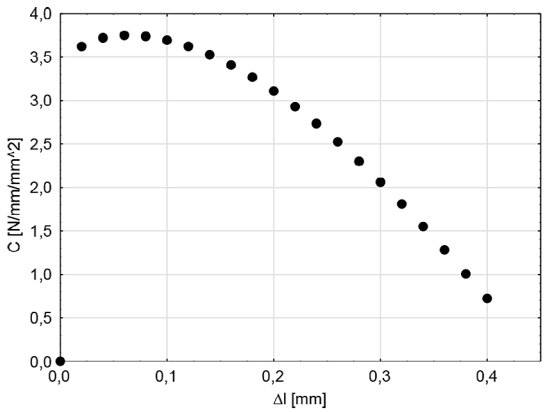

Figure 7. Change in the static stiffness values for the H-specimen type under tensile force

Table 3. Calculated values of the static stiffness for the A and H-type joints

Mean value of the static stiffness C_M [N/mm/mm^2]	A-type joint	H-type joint
	107.21	2.68

Figure 8. Drop tower

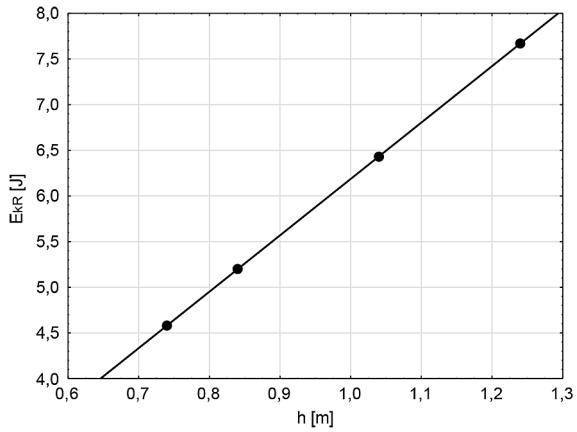

Figure 9. Reverser energy for drop different height values

changes in elongation values (Figures 8, 9). The reverse free-drop analysis from the initial height h allowed the transformation of potential energy (E_p) into kinetic energy, which reached its maximum at the moment of contact between the impactor and the specimen. The process was captured with a Chronos high-speed camera (Figure 10). The specimen elongation (Δx) was recorded using three marker points located in the measurement region of the specimen, Figure 11. The dynamic stiffness K was related to transforming the reverse kinetic energy E_{kR1} into work E_{pS}:

$$E_{kR1} = \frac{1}{2} m_R V_{R1}^2 \tag{4}$$

$$E_{pS} = \frac{1}{2} K \Delta x_{max}^2 \tag{5}$$

and in consequence:

$$E_{kR1} = E_{pS} \Longrightarrow K = \frac{m_R V_{R1}^2}{\Delta x_{max}^2} \tag{6}$$

where: m_R is reverser mass, V_{R1} is reverser initial velocity and

$$\Delta x_{max} = max\left(\Delta x_{free} - \Delta x_{fixed}\right) \tag{7}$$

the extension maximum value between two markers. The procedure for calculating the dynamic stiffness values is presented in Table 4.

The calculated dynamic stiffness values for the A- and H-type adhesive joints, obtained for different dropping heights and initial velocities of the reverser, are presented in Tables 4 and 5 and illustrated in Figures 12, 13 and 14.

To determine the energy at bond-line delamination, the reverser's initial velocity V_{R1} and final velocity V_{R2} measured immediately after fracture, were included in the analysis to determine the energy at bond-line delamination (Figure 15).

Because a portion of the reverser's initial kinetic energy is converted into delamination work, it can be expressed as follows:

$$W_b = \Delta E_p + E_{kR1} - E_{kR2} \tag{8}$$

where: E_{kR1} and E_{kR2} are respectively the initial and final reverser kinetic energy, and

$$\Delta E_p = m_R g \Delta x_b \tag{9}$$

is an increment of reverser potential energy due to displacement.

The results for the A-type adhesive joint are shown in Figure 16, while the calculation procedure and outcomes are presented in Table 6. The

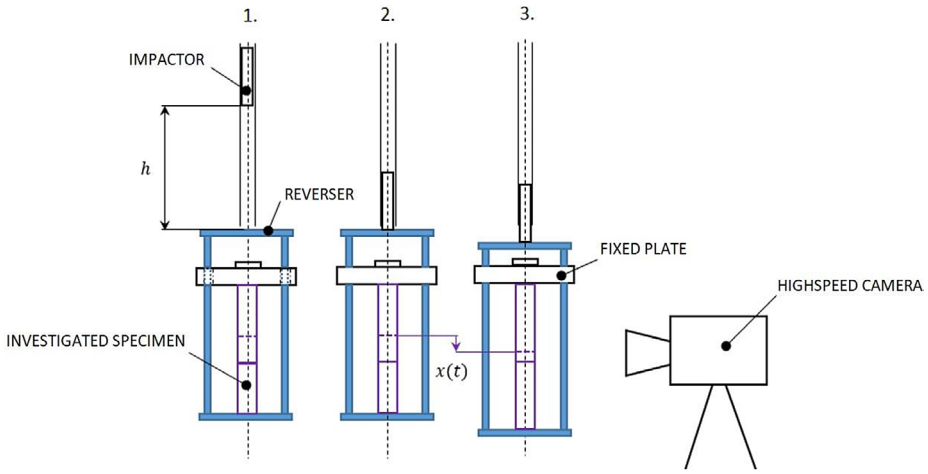

Figure 10. Dynamic test details

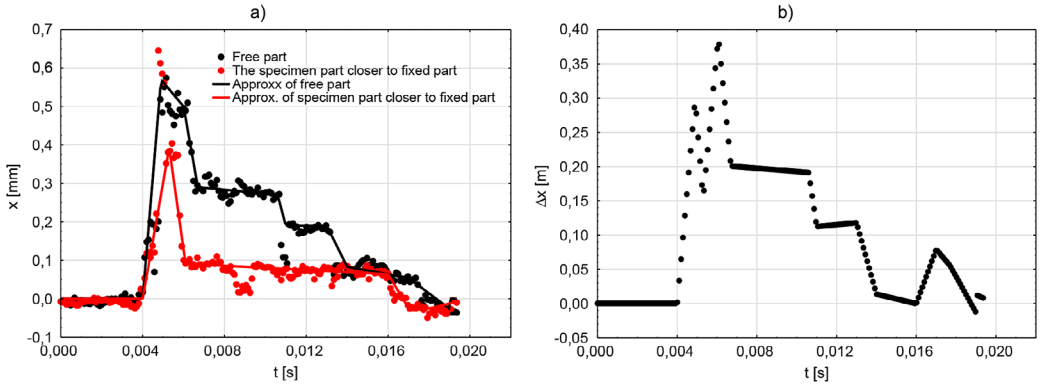

Figure 11. The A joint type's results – impactor height H = 740 mm

Table 4. Dynamic stiffness for the A-joint type

Type of glue: A				
Mass m [kg]		Impactor's high	Reverser's initial velocity	The dynamic stiffness mean value
Impactor	Reverser	h [mm]	V_R [m/s]	[N/mm/mm^2]
1.057	4.1	0.74	1.49	137.3
		0.84	1.59	143.88
		1.04	1.77	156.57
		1.24	1.93	240.9

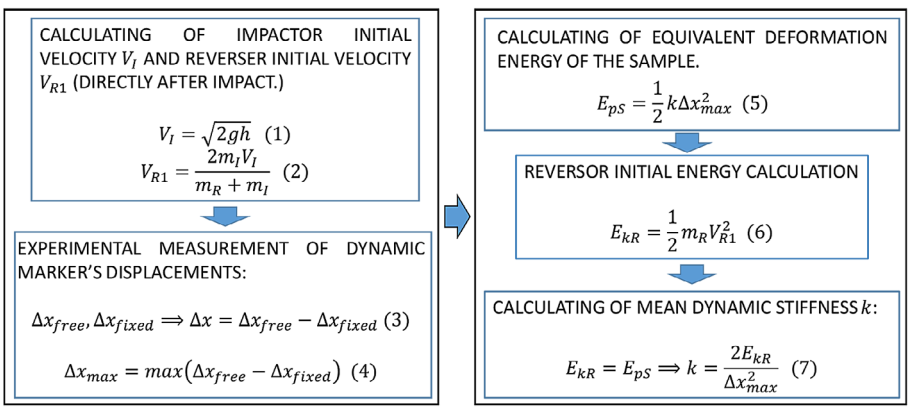

Figure 12. Dynamic stiffness values scheme calculation

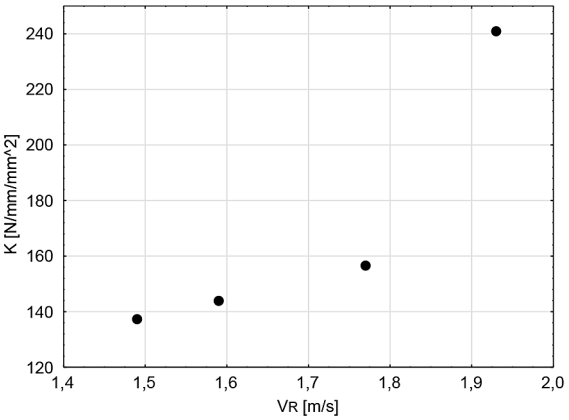

Figure 13. Dynamic stiffness as a function of the reverser's initial velocity – the A-joint type

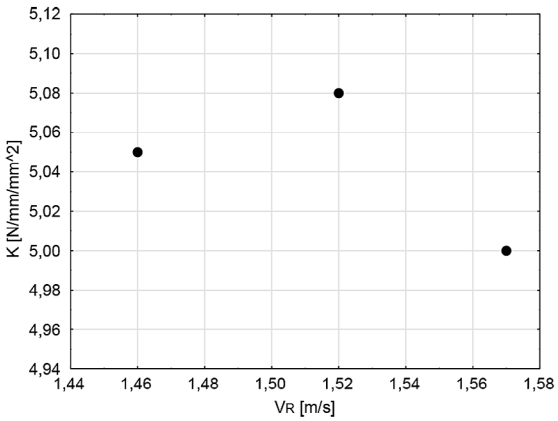

Figure 14. The dynamic stiffness as a function of the reverser's initial velocity – the H-joint type

Table 5. Dynamic stiffness for the H-joint type

Type of glue: H				
Mass m [kg]		Impactor's high	Reverser's initial velocity	The dynamic stiffness mean value
Impactor	Reverser	h [mm]	V_R [m/s]	[N/mm/mm^2]
1.057	4.1	0.65	1.46	5.05
		0.7	1.52	5.08
		0.75	1.57	5

Table 6. The dynamic stiffness mean value for the H glue joint type

A glue black			
Physical quantity name	Symbol and its unit	Pattern	Value
Impactor mass	m_1 [g]	Set value >>	3780
Reverser mass	m_g [g]	Set value >>	4100
Drop height	H [m]	Set value >>	1.24
Bonding area	S [mm^2]	Set value >>	465.82
Impact velocity	V_1 [m/s]	$(2 \cdot 9.81 \cdot h)^{0.5}$	4.93
Reverser velocity after contact	V_{R1} [m/s]	$2\ m_B\ V_B / (m_R + m_B)$	4.73
Reverser velocity at the bursting	V_{R2} [m/s]	Reading >>	3.17
Reverser displacement at the bursting	Δx_r [mm]	Reading >>	0.94
Reverser energy at the impact time	E_{kR1} [J]	$0.0005\ m_R\ V_{R1}^2$	45.91
Reverser energy at the bursting	E_{kR2} [J]	$0.0005\ m_R\ V_{R2}^2$	20.61
Change in the reverser potential energy value	ΔE_{p_R} [J]	$0.000001\ m_R\ g\ \Delta x_r$	0.04
Remarks:	Specimen destruction burst		
Specimen destruction work	W [J]	$\Delta Ep\_R-(E_{kR2}-E_{kR1})$	25.34
Specimen destruction work per unit surface	W* [J/mm^2]	W/S	0.05439

final value of the delamination work per unit area was 0.0549 J/mm^2.

The results obtained in this study provide new insights into the performance of adhesive overlay joints subjected to both static and dynamic loading conditions. A clear distinction was observed between the mechanical response of the joints bonded with DP490 and those bonded with Hybrid CX80, which highlights the importance of adhesive selection for engineering applications where loading conditions vary significantly.

The static tensile tests confirmed that DP490 adhesive produced substantially higher static stiffness compared to CX80. This outcome reflects

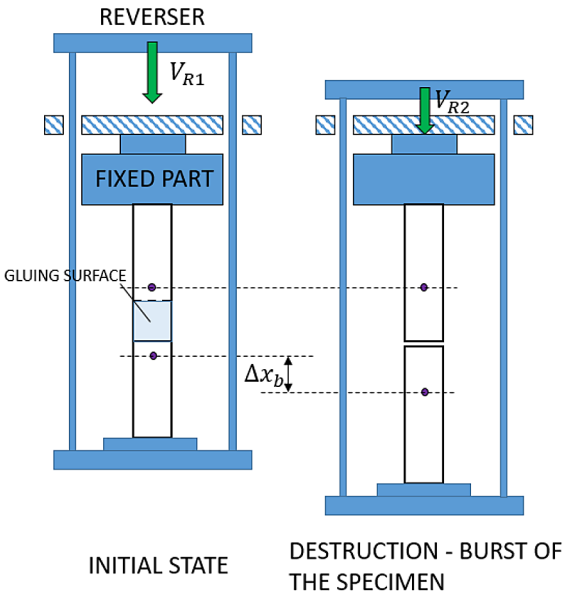

Figure 15. The manner of energy/work at delamination

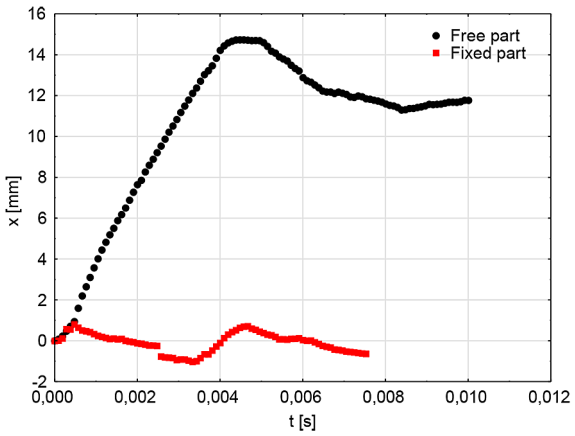

Figure 16. Dynamic displacement changes of the fixed and free parts of the A-specimen type

the structural designation of DP490, which is optimised for demanding conditions, including elevated temperatures and heavy mechanical loads. In contrast, the CX80 adhesive, although more versatile and widely applicable across materials, demonstrated limited resistance under static tensile loading. These findings indicate that adhesives specifically designed for structural purposes generally outperform multipurpose or commercial-grade adhesives in terms of strength and durability.

Under dynamic loading, however, the results revealed a more complex behaviour. The DP490 joints not only retained their mechanical superiority but also showed a notable increase in dynamic stiffness with rising impact velocities. This suggests that the adhesive's intrinsic toughness and ability to dissipate energy improve under high strain rates. The measured delamination work for DP490 further supports this interpretation, as the adhesive was able to sustain significant energy absorption before complete failure. By contrast, the CX80 adhesive exhibited nearly constant dynamic stiffness, approximately double its static value, but without further gains at higher loading energies. Such behaviour may be attributed to the adhesive's more brittle failure mechanism and lower capacity to redistribute stresses across the bonded interface.

The comparison of static and dynamic responses across adhesives emphasises that mechanical performance cannot be generalised from one loading regime to another. For DP490, dynamic testing revealed capacities that exceeded static performance, demonstrating that adhesives classified as high-strength can exploit strain-rate effects to their advantage. For CX80, dynamic results confirmed some improvement over static strength, but the lack of rate sensitivity imposes clear limitations on its use in safety-critical applications where sudden impacts or crash events are likely. These distinctions highlight the importance of complementary testing methods, as neglecting dynamic evaluation may lead to an incomplete understanding of adhesive joint reliability.

Another noteworthy aspect is the diagnostic potential of the proposed testing methodology. By correlating stiffness and elongation values, the study offers a straightforward way to assess the health of bonded joints. This approach could be particularly valuable in industrial diagnostics, where non-destructive methods are often limited in identifying early-stage decohesion. Moreover, the quantitative evaluation of delamination energy highlights the potential of the drop-tower method not only as a characterisation tool but also as a reference for modelling adhesive fracture in numerical simulations.

Overall, the findings expand the current knowledge of bonded joint performance by bridging the gap between static and dynamic characterisation. The differences between adhesives underscore that engineering practice requires a careful match between material properties and operational conditions. For structural and automotive applications where impact resistance is critical, DP490 emerges as a more suitable

adhesive, whereas CX80 may remain appropriate for general-purpose applications with moderate demands. Future research should address the influence of environmental factors, such as temperature, cycling loading and humidity, under combined static–dynamic regimes. In addition, further investigation of microstructural failure mechanisms using advanced imaging techniques could provide deeper insight into the observed differences in performance between adhesives in performance between adhesives.

CONCLUSIONS

The results indicated:

- static and dynamic tests at an analytical approach for stiffness changes enable capturing of differences in the adhesive joints' behaviour for their application;
- the static stiffness of bonded joints is strongly influenced by the adhesive type, reflecting the sensitivity of the bonded region to the applied loading;
- in dynamic loading, the A-type joint exhibited increased dynamic stiffness with higher impactor velocities, surpassing its static one. In contrast, the H-type joint maintained a nearly constant dynamic stiffness, approximately twice its static value;
- the applied energy analysis allowed for a quantitative assessment of delamination energy, highlighting the importance of considering the ratio of mechanical quantities, such as capacity or work, to the bonded region when evaluating joint performance. These findings suggest that both adhesive selection and loading conditions critically affect joint behaviour, emphasising the need for tailored testing approaches depending on the operational scenario.

REFERENCES

1. Yang X., Xia Y., Zhou Q, Wang P.-Ch., Wang K. Modeling of high strength steel joints bonded with toughened adhesive for vehicle crash simulations. International Journal of Adhesion & Adhesives 2012; 39: 21–32. http://dx.doi.org/10.1016/j.ijadhadh.2012.06.007
2. Gollins K., Elvin N., Delale F. Characterization of adhesive joints under high-speed normal impact: Part I – Experimental studies. International Journal of Adhesion & Adhesives 2020; 98: 102529. https://doi.org/10.1016/j.ijadhadh.2019.102529
3. Komorek A. and Godzimirski J. Modified pendulum hammer in impact tests of adhesive, riveted and hybrid lap joints, Journal of Adhesion & Adhesives 2021; 104: 102734.
4. Balkova R., Binar T., Svarc J., Mikulikova R., Dostal P. The influence of temperature and cyclic loading on adhesion in polycarbonate-polyurethane-glass adhesive joint. Journal of Adhesion & Adhesives 2019; 33(13). https://doi.org/10.180/01694243.2019.1575602
5. Kolář V., Műller M., Tichý M., Mishra R.K., Hrabe P., Hanušová K., Hromasova M. Experimental investigation of wavy-lap bonds with natural cotton fabric reinforcement under cyclic loading. Polymers 2021; 13: 2872. https://doi.org/10.3390/polym13172872
6. Sahin R. and Akpinar S. The effects of adherend thickness on the fatigue strength of adhesively bonded single-lap joints. International Journal of Adhesion & Adhesives 2021; 107: 102845. https://doi.org/10.1016/j.ijadhadh.2021.102845
7. Kałuża M. and Hulimka. Methacrylate adhesives to create CFRP laminate-steel joints – preliminary static and fatigue tests. Procedia Engineering. 2017; 172: 489–496. https://doi.org/10.1016/j.proeng.2017.02.057
8. Tichý M., Kolar V., M., Műller, Mishra R.K., Šleger V., Hromasová. Quasi-static shear test of hybrid adhesive bonds based on treated cotton-epoxy resin layer. Polymers 2020; 12: 2945. https://doi.org/10.3390/polym12122945
9. Kowal M. Effect of adhesive joint end shapes on the ultimate load-bearing capacity of carbon fibre-reinforced polymer/steel bonded joints. Advances in Science and Technology Research Journal 2021; 15(4): 299–310 https://doi.org/10.12913/22998624/142370
10. Bula A., Kozłowski M., Hulimka J., Chmielnicki B. Analysis of methyl methacrylate adhesive (MMA) relaxation with non-linear stress–strain dependence. International Journal of Adhesion and Adhesives 2019; 94: 40–46. https://doi.org/10.1016/j.ijadhadh.2019.05.011
11. Xu M., Huang G., Feng S., McShane G., Stronge W. Static and dynamic properties of semi-crystalline polyethene. Polymers 2016; 8(77): 3-14. https://doi.org/10.3390/polym8040077
12. Volkov, G., Logachev, A., Granichin, N., Zhao, Y.-P., Zhang, Y., Petrov, Y. The influence of background ultrasonic field on the strength of adhesive zones under dynamic impact loads. Materials 2021; 14: 3188. https://doi.org/10.3390/ma14123188
13. Maurel-Pantel A., Voisin M., Mazerolle F., Lebon F. Comparison of three different adhesive joints using static and dynamic impact tests: Development

of a new drop weight impact test rig incorporating a modified Arcan fixture. International Journal of Adhesion & Adhesives 2022; 114: 103104. https://doi.org/10.1016/j.ijadhadh.2022.103104

14. Rahman A.R.A., Thin and rectangular die bond pick-up mechanism to reduce cracking during the integrated circuit assembly process, Advances in Science and Technology Research Journal 2020; 14(3): 57–64. https://doi.org/10.12913/22998624/123779
15. Suder J., Vocetka M., Kot T., Fojtík F., Fusek M. Testing of glued joints on plastic parts manufactured using FFF technology. Acta Polytechnica 2020; 60(6): 512–517. https://doi.org/10.14311/AP.2020.60.0512
16. Komorek A. and Godzimirski J. Modified pendulum hammer in impact tests of adhesive, riveted and hybrid lap joints. International Journal of Adhesion & Adhesives 2021; 104: 102734. https://doi.org/10.1016/j.ijadhadh.2020.102734
17. Cao A.S., Houen M., Frangi A.. Impact loading of glued laminated timber beams without finger-joints. Computers and Structures 2024; 296: 107278. https://doi.org/10.3929/ethz-b -000585619
18. Kałuża, M., Hulimka, J., Bula, A. FEM analysis as a tool to study the behavior of methacrylate adhesive in a full-scale steel-steel shear joint. Materials 2022; 15: 330. https://doi.org/10.3390/ma15010330
19. The automotive aluminum manual, 2013, European Aluminium Association, 84 pages.
20. Crash Test Technology International Journal, 20th Anniversary, 2024, 2–4.
21. ASTM D1002-10. Standard Test Method for Apparent Shear Strength of Single-Lap-Joint Adhesively Bonded Metal Specimens by Tension Loading (Metal-to-Metal). 2019, 6 pages.
22. ISO 4587. Adhesives – Determination of tensile lap-shear strength of rigid-to-rigid bonded assemblies. 2003, 4 pages.
23. Scotch-Weld EPX Adhesive DP490, 1996, 4 pages.
24. Bonding composite parts to multiple materials 3M™ Scotch-Weld™ Structural Adhesives, 3M 2017, J392599. CJ1248, 11 pages.
25. CX80 HYBRICX PREMIUM, 2018, 1 page.